I. TO DO

1. Arnoldi

- More analysis on current approximate edge states
- Calculate lifetime of approximate edge states
- Continue analysis of $\log(\mathcal{W})$.

2. Lanczos

- b_n sensitivity to branch cut
- H_K snsitivity to starting time for period.

II. ARNOLDI METHOD

Instead of $\mathcal{L}$, we now have $\mathcal{W}$:

$$\mathcal{W}|O) = U^\dagger \hat{O} U \tag{1}$$

$$\mathcal{W}^n|O) = U(n)^\dagger \hat{O} U(n). \tag{2}$$

We note that $\mathcal{W}$ is unitary,

$$\mathcal{W}^\dagger \mathcal{W}|O) = U(U^\dagger \hat{O} U)U^\dagger \tag{3}$$

$$= \hat{O} = \mathcal{W}\mathcal{W}^\dagger|O). \tag{4}$$

Since $\mathcal{W}$ is unitary, we will see that the Lanczos algorithm will no longer produce a simple tri-diagonal matrix (needs Hermiticity for that). We now outline the Arnoldi method, which reduces to the Lanczos method in the event $\mathcal{W}$ is Hermitian.

Let $|1) = \sigma_1^x$, then assuming we have found the orthonormal basis vectors, $|n), |n-1), \ldots$, then we find $|n+1)$ by time evolving and projecting out the overlaps with the known basis vectors,

$$|n+1') = \mathcal{W}|n) - \sum_{l=1}^{n} |l)(l|\mathcal{W}|n) = \mathcal{W}|n)) - \sum_{l=1}^{n} w_{l,n}|l) \tag{5}$$

$$= \left[1 - \sum_{l=1}^{n} |l)(l|\right] \mathcal{W}|n) = P_n \mathcal{W}|n). \tag{6}$$

We then normalize $|n+1')$,

$$|n+1) = \frac{|n+1')}{\sqrt{(n+1'|n+1')}}. \tag{7}$$

We note,

$$(n+1'|n+1') = (n+1'|P_n\mathcal{W}|n) = (n+1'|\mathcal{W}|n) \tag{8}$$

$$= \sqrt{(n+1'|n+1')}(n+1|\mathcal{W}|n) \tag{9}$$

$$\Rightarrow \sqrt{(n+1'|n+1')} = (n+1|\mathcal{W}|n) = w_{n+1,n}. \tag{10}$$

Thus we start with $|1)$, find $\mathcal{W}|1)$ and $(1|\mathcal{W}|1) = w_{1,1}$, then find the unnormalized $|2') = \mathcal{W}|1) - w_{1,1}|1)$. Then we have $(2'|2') = w_{2,1}^2$. This first step fills in the first two rows of the first column of $\mathcal{W}$ in the Arnoldi basis.

Flipping the equations around, we have,

$$\mathcal{W}|n) = w_{n+1,n}|n+1) + \sum_{l=1}^{n} w_{l,n}|l). \tag{11}$$

As we iterate through this Arnoldi algorithm, we will find the matrix elements of $\mathcal{W}$,

$$\mathcal{W} = \begin{pmatrix} w_{1,1} & w_{1,2} & \ldots \\ w_{2,1} & w_{2,2} & \ldots \\ 0 & w_{3,2} & \ldots \\ 0 & 0 & \ddots \end{pmatrix} \tag{12}$$

Just as for $\mathcal{L}$, the iteration must be cut short after N steps. We call the resulting matrix $\mathcal{W}_N$. Note that $\mathcal{W}_N$ will not be unitary. For $n < N$ we have solved for the dynamics of $A_\infty(nT)$ exactly,

$$A_\infty(nT) = (1|\mathcal{W}^n|1) \sim (1|\mathcal{W}_N^n|1). \tag{13}$$

For dynamics generated by $\mathcal{W}_N$, we call the corresponding $A_\infty = A_\infty^N$.

It turns out that $A_\infty^N \sim A_\infty$ for $n \gg N$ for many situations involving 0-π ASMs. This is a good indication that we can repeat the same story of the previous paper.

We note that for the last state $|N)$ we have,

$$\mathcal{W}|N) = \sum_{l=1}^{N} w_{l,N}|l) + w_{N+1,N}|N+1), \tag{14}$$

and by stopping at $|N)$, we are making some form of a Markov approximation at a rate of $w_{N+1,N}$. Thus we expect almost all dynamics produced by $\mathcal{W}_N$ to eventually decay.

A. High frequency limit

Now we let $T \to 0$, we have to first order in T,

$$\mathcal{W}|1) \sim |1) + iT\mathcal{L}|1), \tag{15}$$

thus we have,

$$|2') = |1) + iT\mathcal{L}|1) - 1|1) = iT\mathcal{L}|1). \tag{16}$$

After normalizing $|2) = w_{2,1}|2')$ we now move onto the next state. To first order in T,

$$\mathcal{W}|2) \sim |2) + iT\mathcal{L}|2), \tag{17}$$

yielding,

$$|3') = |2) + iT\mathcal{L}|2) - 1|2) - (1|\mathcal{L}|2)|1) = iT\mathcal{L}|2) - (1|\mathcal{L}|2)|1). \tag{18}$$

As $|3')$ and all higher $|n > 3)$ are determined from $\mathcal{L}$ alone, we expect high-frequency Arnoldi to reduce to Lanczos.

B. Free case

Recall that in the free case we have,

$$U = e^{-i\frac{T}{2}J_x H_{xx}} e^{-i\frac{T}{2}gH_z}, \tag{19}$$

and,

$$U^\dagger \vec{a} U = M\vec{a}. \tag{20}$$

where the vector of majoranas, $\vec{a}$, is

$$\vec{a} = \begin{pmatrix} a_{odd} \\ a_{even} \end{pmatrix}, \tag{21}$$

and M is,

$$M = \left(\begin{array}{cccc|cccc} a' & & & & c' & & & \\ b & a & & & -d & c & & \\ & \ddots & \ddots & & & \ddots & \ddots & \\ \hline -c & d & & & a & b & & \\ & \ddots & \ddots & & & \ddots & \ddots & \\ & & -c' & & & & a' & \end{array}\right), \tag{22}$$

with

$$a = \cos(Tg)\cos(TJ_x),\ b = \sin(Tg)\sin(TJ_x), \tag{23}$$
$$c = -\sin(Tg)\cos(TJ_x),\ d = -\cos(Tg)\sin(TJ_x), \tag{24}$$
$$a' = \cos(Tg),\ c' = -\sin(Tg). \tag{25}$$

M is orthogonal, and can admit eigenvalues at ± 1 depending on the parameters. Starting with the initial state $\sigma_1^x = a_1$, we repeat the above Arnoldi algorithm by simply replacing $\mathcal{W}$ with M. This will produce a single-particle $\mathcal{W}$ that can fully span the Krylov space of σ_1^x in the free case, preferable over the full many-body basis of the spin basis.

Fig. 1 shows the comparison of M of Eq. 22 to the rotated basis $\mathcal{W}$. In particular, Fig. 1 takes $H_W = \log(\mathcal{W})$ and truncates around the central diagonal and the corners to give H'_W, and exponentiates to yield $\mathcal{W}'$. Fig. 1 compares this to the exact solution.

Fig. 2 shows the comparison of $\mathcal{W}$ and $\log(\mathcal{W})$ when interactions are turned on. The first two rows of Fig. 2 show the free limit. In all cases, we stop the calculation at $N = 2L$, which is where the algorithm terminates for the free case regardless. As we move down the rows, we turn on the interactions from very small to moderate. The matrix $\mathcal{W}$ transforms in a predictable manner and the physics of the edge of Krylov space remains local without long range couplings. However, H_W is a different story. Already in the free case, there are long ranged hoppings present for the π-modes. As the interactions are turned on, many long-ranged hoppings to the last calculuated Krylov basis vector at $N = 2L$ are turned on. Their strength in fact dominates the SSH model that resides along the main diagonal.

The intuition built up from the $\mathcal{W}$ carries over from the free case to the interacting case. However, H_W varies wildly as J_z is turned on and appears to be sensitive to the value of N.

In both Fig. 1 and 2, we have,

$$\mathcal{W} \sim e^{H_W}, \tag{26}$$

where, H_W is a real anti-symmetric matrix,

$$H_W^T = -H_W. \tag{27}$$

Of course, we can rewrite this as,

$$\mathcal{W} \sim e^{-iH'_W} \tag{28}$$

where H_W is a Hermitian matrix with purely complex hoppings.

In many examples of Fig. 1 and 2, we have a strong diagonal, which corresponds to an SSH model with alternating strong and weak hopping strengths. In the event of a π-mode phase, we have a strong non-local hoppping $h_{1,L}$. We have,

$$H_0 = H^{(1,L)}_{\text{SSH topo}} \tag{29}$$
$$H_\pi = H^{(2,L-1)}_{\text{SSH triv}} + ihc_1^\dagger c_L - ihc_L^\dagger c_1 \tag{30}$$
$$H_{0,\pi} = H^{(2,L-1)}_{\text{SSH topo}} + ihc_1^\dagger c_L - ihc_L^\dagger c_1 \tag{31}$$
$$H_{\text{triv}} = H^{(1,L)}_{\text{SSH triv}}. \tag{32}$$

C. Approximate SM calculation

We can solve for the left eigenvectors of $\mathcal{W}$ which allows us to work from the first site and iterate into the bulk.

We can solve for the left eigen vectors of $\mathcal{W}$ by simply setting $\psi_1 = 1$, setting $\lambda = \pm 1$ and iterating. Taking the inner product of the left eigenvector onto the first column of the matrix $\mathcal{W} - \lambda$, we have,

$$\psi_1 = 1 \tag{33}$$
$$\Rightarrow \psi_2 = \frac{w_{1,1} - \lambda}{w_{2,1}}. \tag{34}$$

Now considering the inner product of the left eigenvector onto the second column of the matrix $\mathcal{W} - \lambda$, we have,

$$w_{1,2}\psi_1 + (w_{2,2} - \lambda)\psi_2 + w_{3,2}\psi_3 = 0 \tag{35}$$
$$\Rightarrow \psi_3 = -\frac{1}{w_{3,2}}\left((w_{2,2} - \lambda)\psi_2 + w_{1,2}\psi_1\right). \tag{36}$$

The pattern is clear for the rest of the eigenvector components,

$$\psi_{n+1} = -\frac{1}{w_{n+1,n}}\left((w_{n,n} - \lambda)\psi_n + \sum_{i=1}^{n-1} w_{i,n}\psi_i\right), \tag{37}$$

with a final normalization step at the end of the calculation.

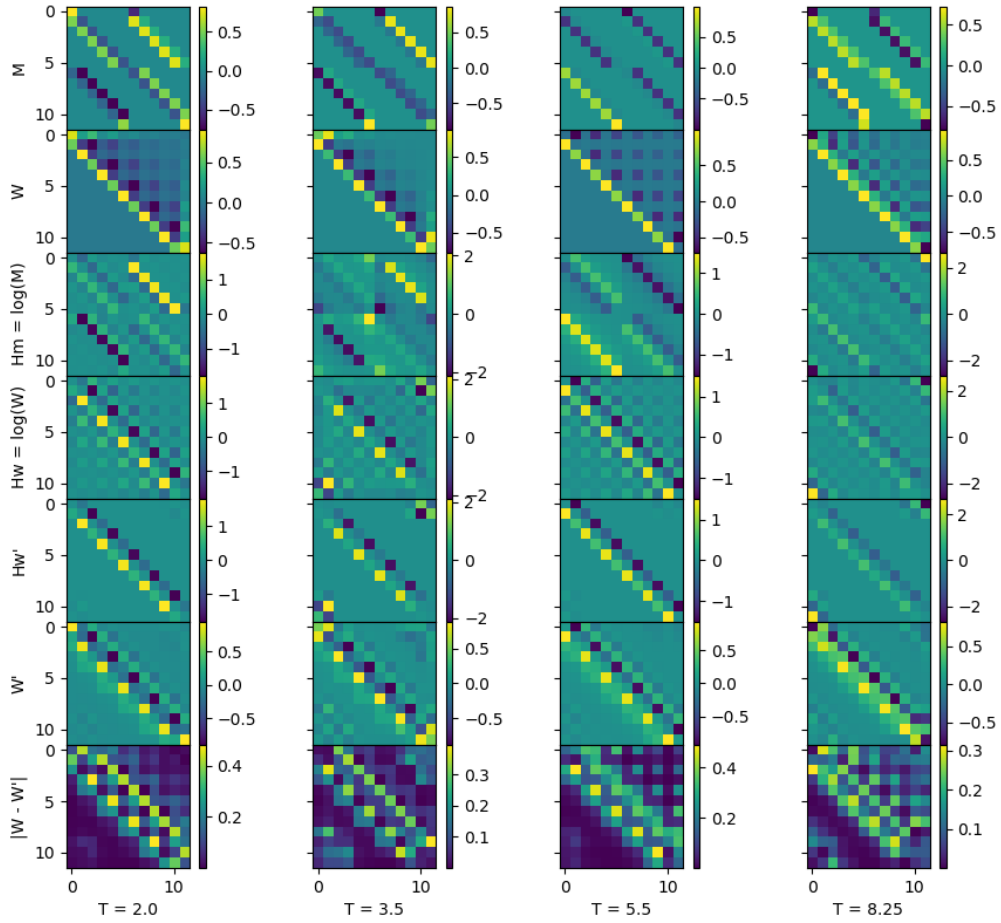

FIG. 1: Free case, in the Majorana basis, comparison of exact $\log(M)$ of Eq (22) and truncation of $\log(\mathcal{W})$ around the central diagonal and the corners.

We can get a rough estimate of the lifetime by noting,

$$e^{-\gamma_{0,\pi}} = |\langle\psi_{0,\pi}|\mathcal{W}|\psi_{0,\pi}\rangle|, \tag{38}$$

which is shown in Fig. 3 to give reasonable estimates for the lifetime.

We can push Eq. (38) a little further with the help of Eq. (37), which we rewrite as,

$$\sum_{i=1}^{n-1}\psi_i w_{i,n} = -\psi_{n+1}w_{n+1,n} - (w_{n,n}-\lambda)\psi_n. \tag{39}$$

Note that the above is the solution of $\langle\psi|\mathcal{W} = \langle\psi|\lambda$ by plugging in for $\psi_1 = 1$ and solving for ψ_{n+1} using knowledge of $\psi_{1\leq l\leq n}$ and the n^{th} column of $\mathcal{W}$. This means that we never consider $\sum_{i=1}^{N}\psi_i w_{i,N}$. If we were actually solving the eigenvalue/vector problem, then this quantity should equal $\lambda\psi_N$, but our method will not yield this. However, we hope that our approximate solution is close enough and emperically agrees with the decay.

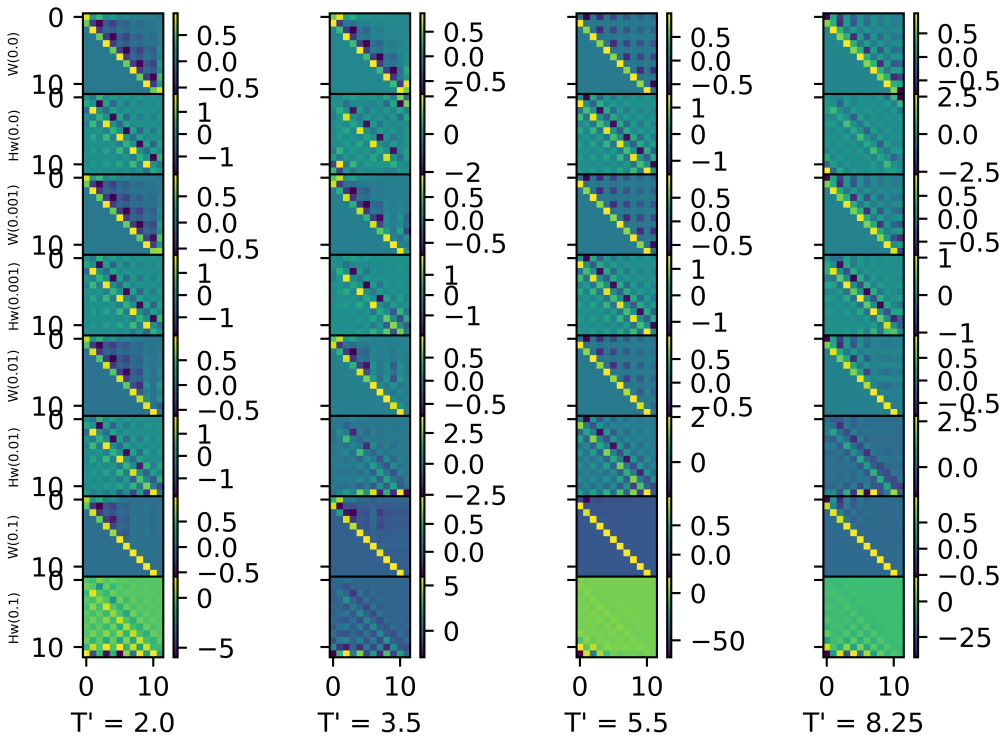

FIG. 2: Interacting analog to Fig. 1. We produce the $\mathcal{W}$ matrices for σ_1^x for a few different values of J_z. We also find the corresponding $H_W = \log(\mathcal{W})$. All Arnoldi algorithms are terminated after $N = 2L$ calculations.

We start by working with the unnormalized ψ_λ as in Eq. (37), we have,

$$\langle\psi_\lambda|\mathcal{W}|\psi_\lambda\rangle = \sum_{k=1}^{N-1}\left[\psi_{k+1}w_{k+1,k} + \psi_k w_{k,k} + \sum_{m=1}^{k-1}\psi_m w_{m,k}\right]\psi_k + \sum_{m=1}^{N}\psi_m w_{m,N}\psi_N \tag{40}$$

$$= \sum_{k=1}^{N-1}\left[\psi_{k+1}w_{k+1,k} + \psi_k w_{k,k} + (-\psi_{k+1}w_{k+1,k} - (w_{k,k}-\lambda)\psi_k)\right]\psi_k + \sum_{m=1}^{N}\psi_m w_{m,N}\psi_N \tag{41}$$

$$= \sum_{k=1}^{N-1}\lambda\psi_k^2 + \sum_{m=1}^{N}\psi_m w_{m,N}\psi_N \tag{42}$$

$$= \lambda\left[\sum_{k=1}^{N}\psi_k^2 + \lambda\sum_{m=1}^{N}\psi_m w_{m,N}\psi_N - \psi_N^2\right]. \tag{43}$$

We normalize $\psi_\lambda \to \psi_\lambda/N_\lambda$,

$$|\langle\psi_\lambda|\mathcal{W}|\psi_\lambda\rangle| = 1 + \frac{\lambda}{N_\lambda^2}\sum_{m=1}^{N}\psi_m w_{m,N}\psi_N - \frac{\psi_N^2}{N_\lambda^2}. \tag{44}$$

Thus we have,

$$\gamma_\lambda \sim \frac{\psi_N^2}{N_\lambda^2} - \frac{\lambda}{N_\lambda^2}\sum_{m=1}^{N}\psi_m w_{m,N}\psi_N. \tag{45}$$

We cannot proceed further without making approximations to $\mathcal{W}$ or to ψ. As it stands, Eq. (45) gives every similar performance to Eq. (38).

Emperically, we find the second term to often be much smaller than the first, we of course require $\gamma > 0$, thus we can approximate it even further as,

$$\gamma_\lambda \sim \frac{\psi_N^2}{N_\lambda^2}. \tag{46}$$

This approximation hardly changes the agreement seen in Fig. 3 for the approximate lifetime.

D. Free $\mathcal{W}$

It is straightforward, but tedious to verify the Arnoldi alogirthm produces the following $\mathcal{W}$ for $L = 4$,

$$\begin{pmatrix} c_1 & -s_1c_2 & s_2s_1c_1 & -s_2s_1^2c_2 & s_2^2s_1^2c_1 & -s_2^2s_1^3c_2 & s_2^3s_1^3c_1 & -s_2^3s_1^4 \\ s_1 & c_2c_1 & -s_2c_1^2 & s_1c_1s_2c_2 & -s_2^2s_1c_1^2 & s_2^2s_1^2c_2c_1 & -s_2^3s_1^2c_1^2 & s_2^3s_1^3c_1 \\ 0 & s_2 & c_2c_1 & -s_1c_2^2 & s_1c_1s_2c_2 & -s_2s_1^2c_2^2 & s_2^2s_1^2c_2c_1 & -s_2^2s_1^3c_2 \\ 0 & 0 & s_1 & c_2c_1 & -s_2c_1^2 & s_1c_1s_2c_2 & -s_2^2s_1c_1^2 & s_2^2s_1^2c_1 \\ 0 & 0 & 0 & s_2 & c_2c_1 & -s_1c_2^2 & s_1c_1s_2c_2 & -s_2s_1^2c_2 \\ 0 & 0 & 0 & 0 & s_1 & c_2c_1 & -s_2c_1^2 & s_1c_1s_2 \\ 0 & 0 & 0 & 0 & 0 & s_2 & c_2c_1 & -s_1c_2 \\ 0 & 0 & 0 & 0 & 0 & 0 & s_1 & c_1 \end{pmatrix}, \tag{47}$$

where we have,

$$c_1 = \cos(Tg) \tag{48}$$
$$c_2 = \cos(T) \tag{49}$$
$$s_1 = \sin(Tg) \tag{50}$$
$$s_2 = \sin(T). \tag{51}$$

For even rows, starting on the column corresponding to the subdiagonal, we have

$$\{s_1,\ c_1c_2,\ -s_2c_1^2,\ (s_1s_2)c_1c_2,\ -(s_1s_2)s_2c_1^2,\ \ldots,\ (s_1s_2)^n(c_1c_2),\ (s_1s_2)^n(-s_2c_1^2),\ \ldots\}. \tag{52}$$

For odd rows, starting on the column corresponding to the subdiagonal, we have

$$\{s_2,\ c_1c_2,\ -s_1c_2^2,\ (s_1s_2)c_1c_2,\ -(s_1s_2)s_1c_2^2,\ \ldots,\ (s_1s_2)^n(c_1c_2),\ (s_1s_2)^n(-s_1c_2^2),\ \ldots\}. \tag{53}$$

For rows or columns at the edge of the matrix, use the above rules and then divide by c_2.

Limit of $g \to 0$ (static zero mode, letting $a = g$) or limit of $g \to 2\pi/T$ (non static zero mode, letting $a = g - 2\pi/T$),

$$\begin{bmatrix} 1 & -Ta\cos(T) & Ta\sin(T) & 0 & 0 & 0 & 0 & 0 \\ Ta & \cos(T) & -\sin(T) & Ta\sin(T)\cos(T) & -Ta\sin^2(T) & 0 & 0 & 0 \\ 0 & \sin(T) & \cos(T) & -Ta\cos^2(T) & Ta\sin(T)\cos(T) & 0 & 0 & 0 \\ 0 & 0 & Ta & \cos(T) & -\sin(T) & Ta\sin(T)\cos(T) & -Ta\sin^2(T) & 0 \\ 0 & 0 & 0 & \sin(T) & \cos(T) & -Ta\cos^2(T) & Ta\sin(T)\cos(T) & 0 \\ 0 & 0 & 0 & 0 & Ta & \cos(T) & -\sin(T) & Ta\sin(T) \\ 0 & 0 & 0 & 0 & 0 & \sin(T) & \cos(T) & -Ta\cos(T) \\ 0 & 0 & 0 & 0 & 0 & 0 & Ta & 1 \end{bmatrix}. \tag{54}$$

Limit of $g \to \pi/T$ (π mode, $a = g - \pi/T$),

$$\begin{bmatrix} -1 & Ta\cos(T) & Ta\sin(T) & 0 & 0 & 0 & 0 & 0 \\ -Ta & -\cos(T) & -\sin(T) & Ta\sin(T)\cos(T) & Ta\sin^2(T) & 0 & 0 & 0 \\ 0 & \sin(T) & -\cos(T) & Ta\cos^2(T) & Ta\sin(T)\cos(T) & 0 & 0 & 0 \\ 0 & 0 & -Ta & -\cos(T) & -\sin(T) & Ta\sin(T)\cos(T) & Ta\sin^2(T) & 0 \\ 0 & 0 & 0 & \sin(T) & -\cos(T) & Ta\cos^2(T) & Ta\sin(T)\cos(T) & 0 \\ 0 & 0 & 0 & 0 & -Ta & -\cos(T) & -\sin(T) & Ta\sin(T) \\ 0 & 0 & 0 & 0 & 0 & \sin(T) & -\cos(T) & Ta\cos(T) \\ 0 & 0 & 0 & 0 & 0 & 0 & -Ta & -1 \end{bmatrix}. \tag{55}$$

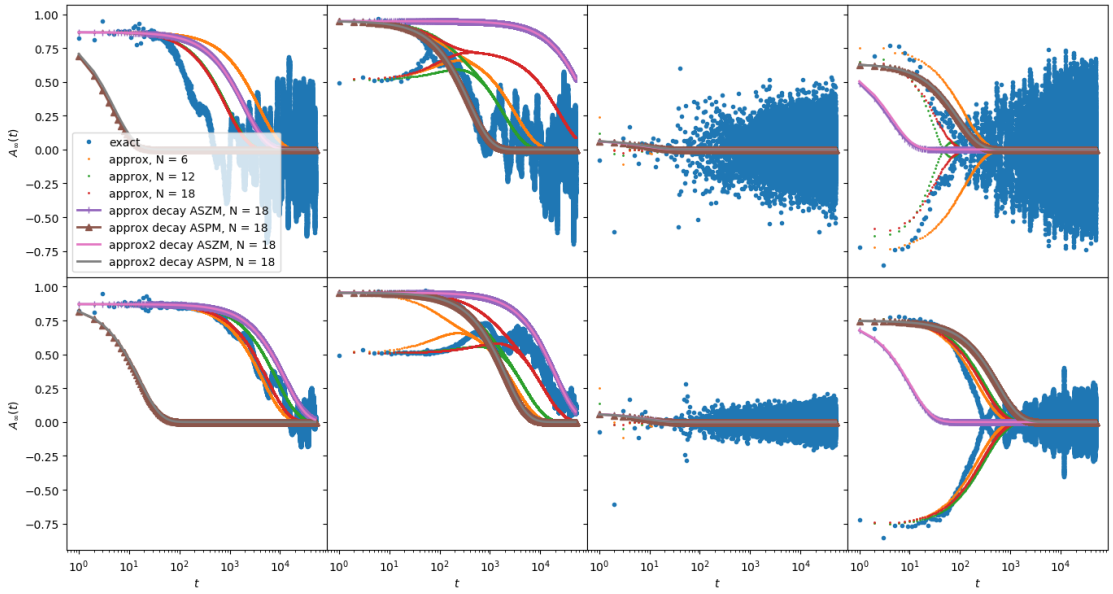

FIG. 3: Time evolution of approximate edge states of $\mathcal{W}$ for an interacting example, compared to exact solution of A_∞ (blue). The top row is for the very small system size of $L = 4$ and the bottom row is for $L = 6$. The four columns compare four different phases, ASZM phase, ASZPM phase, trivial phase, ASPM phase. The dimension of $\mathcal{W}_N$ is given as either $N = 6, 12, 18$. The approximate data sets are $|\psi(nT)\rangle \sim \psi_{0,1}|\psi_0(nT)\rangle + \psi_{\pi,1}|\psi_\pi(nT)\rangle)$, where $|\psi_{0,\pi}(nT)\rangle = \mathcal{W}^n|\psi_{0,\pi}\rangle$, with $\psi_{0,\pi}$ being the approximate edge modes and $\psi_{0/\pi,1}$ being the first elements and thus we are approximating $U \sim |\psi_0\rangle\langle\psi_0| + |\psi_\pi\rangle\langle\psi_\pi|$. In all cases, we see the approximate data sets do a good job of recreating the dynamics, well beyond N, where the dynamics is no longer guarenteed to be exact. Futher, truncation of the Arnoldi method gives a natural way to introduce decay into the problem.

Limit of $T \to \pi$ ($0, \pi$ mode, $a = T - \pi$),

$$\begin{bmatrix}
-ag\sin(\pi g)+\cos(\pi g) & ag\cos(\pi g)+\sin(\pi g) & -\frac{a\sin(2\pi g)}{2} & -a\sin^2(\pi g) & 0 & 0 & 0 & 0 \\
ag\cos(\pi g)+\sin(\pi g) & ag\sin(\pi g)-\cos(\pi g) & a\cos^2(\pi g) & a\sin(\pi g)\cos(\pi g) & 0 & 0 & 0 & 0 \\
0 & -a & ag\sin(\pi g)-\cos(\pi g) & -ag\cos(\pi g)-\sin(\pi g) & a\sin(\pi g)\cos(\pi g) & a\sin^2(\pi g) & 0 & 0 \\
0 & 0 & ag\cos(\pi g)+\sin(\pi g) & ag\sin(\pi g)-\cos(\pi g) & a\cos^2(\pi g) & a\sin(\pi g)\cos(\pi g) & 0 & 0 \\
0 & 0 & 0 & -a & ag\sin(\pi g)-\cos(\pi g) & -ag\cos(\pi g)-\sin(\pi g) & a\sin(\pi g)\cos(\pi g) & -a\sin^2(\pi \\
0 & 0 & 0 & 0 & ag\cos(\pi g)+\sin(\pi g) & ag\sin(\pi g)-\cos(\pi g) & a\cos^2(\pi g) & -\frac{a\sin(2\pi} \\
0 & 0 & 0 & 0 & 0 & -a & ag\sin(\pi g)-\cos(\pi g) & ag\cos(\pi g)+s \\
0 & 0 & 0 & 0 & 0 & 0 & ag\cos(\pi g)+\sin(\pi g) & -ag\sin(\pi g)+
\end{bmatrix} \tag{56}$$

Focusing on the first matrix for now, we can perform a rotation, on the 2×2 subblocks that look like rotations of angle T. We rotate on the $(2, 3)$ (row/column) subspace (along with $(3, 4)$, $(5, 6)$, etc.) with

$$\begin{bmatrix}
1 & 0 & 0 & 0 & 0 & 0 & 0 & 0 \\
0 & \frac{\sqrt{2}}{2} & \frac{\sqrt{2}}{2} & 0 & 0 & 0 & 0 & 0 \\
0 & \frac{\sqrt{2}i}{2} & -\frac{\sqrt{2}i}{2} & 0 & 0 & 0 & 0 & 0 \\
0 & 0 & 0 & \frac{\sqrt{2}}{2} & \frac{\sqrt{2}}{2} & 0 & 0 & 0 \\
0 & 0 & 0 & \frac{\sqrt{2}i}{2} & -\frac{\sqrt{2}i}{2} & 0 & 0 & 0 \\
0 & 0 & 0 & 0 & 0 & \frac{\sqrt{2}}{2} & \frac{\sqrt{2}}{2} & 0 \\
0 & 0 & 0 & 0 & 0 & \frac{\sqrt{2}i}{2} & -\frac{\sqrt{2}i}{2} & 0 \\
0 & 0 & 0 & 0 & 0 & 0 & 0 & 1
\end{bmatrix} \tag{57}$$

normalsize so that we have $V^\dagger \mathcal{W} V$. The end result is,

$$\begin{bmatrix}
1 & -\frac{\sqrt{2}Tae^{-iT}}{2} & -\frac{\sqrt{2}Tae^{iT}}{2} & 0 & 0 & 0 \\
\frac{\sqrt{2}Ta}{2} & e^{-iT} & 0 & \frac{Ta\left((\sin(2T)+i\cos(2T))e^{2iT}+i\right)e^{-2iT}}{4} & \frac{Ta\sin(2T)}{4}+\frac{iTa\cos(2T)}{4}+\frac{iTa}{2}-\frac{iTae^{-2iT}}{4} & 0 \\
\frac{\sqrt{2}Ta}{2} & 0 & e^{iT} & \frac{Ta\left(ie^{2iT}+\sin(2T)-i\cos(2T)-2i\right)}{4} & \frac{Ta\left(-ie^{2iT}+\sin(2T)-i\cos(2T)\right)}{4} & 0 \\
0 & \frac{iTa}{2} & -\frac{iTa}{2} & e^{-iT} & 0 & \frac{Ta\sin(2T)}{4}+\frac{iTa\cos(2T)}{4}+\frac{iTae^{-2i}}{4} \\
0 & \frac{iTa}{2} & -\frac{iTa}{2} & 0 & e^{iT} & \frac{Ta\left(-i\left(1-e^{2iT}\right)+\sin(2T)-2i\cos^2(T)\right.}{4} \\
0 & 0 & 0 & \frac{iTa}{2} & -\frac{iTa}{2} & e^{-iT} \\
0 & 0 & 0 & \frac{iTa}{2} & -\frac{iTa}{2} & 0 \\
0 & 0 & 0 & 0 & 0 & \frac{\sqrt{2}iTa}{2}
\end{bmatrix} \tag{58}$$

We make the ansatz for the edge mode to be $\psi \sim (a^0\phi_1, a\phi_2, a\phi_3, a^2\phi_4, a^2\phi_5, \dots)$, the end result is,

$$\psi = \begin{bmatrix}
1 \\
-\frac{\sqrt{2}Ta}{2\left(-1+e^{-iT}\right)} \\
-\frac{\sqrt{2}Ta}{2\left(e^{iT}-1\right)} \\
-\frac{\sqrt{2}T^2a^2}{4\left(-1+e^{-iT}\right)\tan\left(\frac{T}{2}\right)} \\
-\frac{\sqrt{2}T^2a^2}{4\left(e^{iT}-1\right)\tan\left(\frac{T}{2}\right)} \\
-\frac{\sqrt{2}T^3a^3}{8\left(-1+e^{-iT}\right)\tan^2\left(\frac{T}{2}\right)} \\
-\frac{\sqrt{2}T^3a^3}{8\left(e^{iT}-1\right)\tan^2\left(\frac{T}{2}\right)} \\
0
\end{bmatrix}, \tag{59}$$

or, $\psi_1 = 1$ and for later elements,

$$\psi_{2n} = -\frac{\sqrt{2}(aT)^n}{2^n(e^{-iT}-1)\tan^{n-1}\left(\frac{T}{2}\right)}, \tag{60}$$

$$\psi_{2n+1} = -\frac{\sqrt{2}(aT)^n}{2^n(e^{iT}-1)\tan^{n-1}\left(\frac{T}{2}\right)}. \tag{61}$$

This ansatz assumes elements ψ_{2n} and ψ_{2n+1} are proportional to a^n and we ignore all contributions for these components that have higher order. We want for our solution to live in the null space of $V^\dagger \mathcal{W} V - \mathbb{I}$, which plugging in for the generic form of ψ, $\psi \sim (a^0\phi_1, a\phi_2, a\phi_3, a^2\phi_4, a^2\phi_5, \dots)$, we arrive at

$$\frac{iTa}{2}\begin{pmatrix}1 & -1\\ 1 & -1\end{pmatrix}\begin{pmatrix}\phi_{2n}\\ \phi_{2n+1}\end{pmatrix} = \begin{pmatrix}e^{-iT}-1 & 0\\ 0 & e^{iT}-1\end{pmatrix}\begin{pmatrix}\phi_{2n+2}\\ \phi_{2n+3}\end{pmatrix}. \tag{62}$$

The rotation V we performed makes this trivial to solve. The boundary condition is,

$$\psi_1 = \phi_1 = 1, \tag{63}$$

and

$$\begin{pmatrix}e^{-iT}-1 & 0\\ 0 & e^{iT}-1\end{pmatrix}\begin{pmatrix}\phi_2\\ \phi_3\end{pmatrix} = \frac{Ta}{\sqrt{2}}\begin{pmatrix}1\\ 1\end{pmatrix}\phi_1 \tag{64}$$

We arrive at similar results for the π mode phase, the rotated matrix,

$$\begin{bmatrix}
-1 & -\frac{\sqrt{2}Tae^{iT}}{2} & -\frac{\sqrt{2}Tae^{-iT}}{2} & 0 & 0 & 0 & 0 & 0 \\
\frac{\sqrt{2}Ta}{2} & -e^{iT} & 0 & \frac{Ta(-\sin(2T)+i\cos(2T))}{2} & \frac{iTa}{2} & 0 & 0 & 0 \\
\frac{\sqrt{2}Ta}{2} & 0 & i\sin(T)-\cos(T) & -\frac{iTa}{2} & -\frac{Ta(\sin(2T)+i\cos(2T))}{2} & 0 & 0 & 0 \\
0 & \frac{iTa}{2} & -\frac{iTa}{2} & -e^{iT} & 0 & \frac{Ta(-\sin(2T)+i\cos(2T))}{2} & \frac{iTa}{2} & 0 \\
0 & \frac{iTa}{2} & -\frac{iTa}{2} & 0 & i\sin(T)-\cos(T) & -\frac{iTa}{2} & -\frac{Ta(\sin(2T)+i\cos(2T))}{2} & 0 \\
0 & 0 & 0 & \frac{iTa}{2} & -\frac{iTa}{2} & -e^{iT} & 0 & \frac{\sqrt{2}Ta(-\sin(} \\
0 & 0 & 0 & \frac{iTa}{2} & -\frac{iTa}{2} & 0 & i\sin(T)-\cos(T) & -\frac{\sqrt{2}Ta(\sin(} \\
0 & 0 & 0 & 0 & 0 & \frac{\sqrt{2}iTa}{2} & -\frac{\sqrt{2}iTa}{2} & -
\end{bmatrix} \tag{65}$$

and the edge mode, starting with $\psi_1 = 1$ and,

$$\psi_{2n} = -\frac{\sqrt{2}(aT)^n}{2^n(-e^{iT}+1)\tan^{n-1}\left(\frac{T}{2}\right)}, \tag{66}$$

$$\psi_{2n+1} = -\frac{\sqrt{2}(aT)^n}{2^n(-e^{-iT}+1)\tan^{n-1}\left(\frac{T}{2}\right)}. \tag{67}$$

To arrive at these results, we now want our solution to live in the null space of $V^\dagger \mathcal{W} V + \mathbb{I}$. Again, plugging in for the generic form of ψ, $\psi \sim (a^0\phi_1, a\phi_2, a\phi_3, a^2\phi_4, a^2\phi_5, \dots)$, we arrive at

$$\frac{iTa}{2}\begin{pmatrix}1 & -1\\ 1 & -1\end{pmatrix}\begin{pmatrix}\phi_{2n}\\ \phi_{2n+1}\end{pmatrix} = \begin{pmatrix}-e^{iT}+1 & 0\\ 0 & -e^{-iT}+1\end{pmatrix}\begin{pmatrix}\phi_{2n+2}\\ \phi_{2n+3}\end{pmatrix}. \tag{68}$$

The boundary condition is now,

$$\psi_1 = \phi_1 = -1, \tag{69}$$

and

$$\begin{pmatrix}-e^{iT}+1 & 0\\ 0 & -e^{-iT}+1\end{pmatrix}\begin{pmatrix}\phi_2\\ \phi_3\end{pmatrix} = \frac{Ta}{\sqrt{2}}\begin{pmatrix}1\\ 1\end{pmatrix}\phi_1 \tag{70}$$

For the $0-\pi$ matrix, the dominant 2×2 subblocks are shifted up by one and modified slightly. Performing the rotation,

$$V = \begin{bmatrix} -\frac{\sqrt{2}\sin(\pi g)}{2\sqrt{\cos(\pi g)+1}} & -\frac{\sqrt{2}\sqrt{1-\cos(\pi g)}\sin(\pi g)}{2(\cos(\pi g)-1)} & 0 & 0 & 0 & 0 & 0 & 0\\ \frac{\sqrt{2}\sqrt{\cos(\pi g)+1}}{2} & \frac{\sqrt{2}\sqrt{1-\cos(\pi g)}}{2} & 0 & 0 & 0 & 0 & 0 & 0\\ 0 & 0 & \frac{\sqrt{2}}{2} & \frac{\sqrt{2}}{2} & 0 & 0 & 0 & 0\\ 0 & 0 & \frac{\sqrt{2}i}{2} & -\frac{\sqrt{2}i}{2} & 0 & 0 & 0 & 0\\ 0 & 0 & 0 & 0 & \frac{\sqrt{2}}{2} & \frac{\sqrt{2}}{2} & 0 & 0\\ 0 & 0 & 0 & 0 & \frac{\sqrt{2}i}{2} & -\frac{\sqrt{2}i}{2} & 0 & 0\\ 0 & 0 & 0 & 0 & 0 & 0 & 1 & 0\\ 0 & 0 & 0 & 0 & 0 & 0 & 0 & 1 \end{bmatrix} \tag{71}$$

on the $0-\pi$ matrix, we arrive at,

$$\begin{bmatrix} -1 & \frac{ag\sin(\pi g)}{\sqrt{1-\cos(\pi g)}\sqrt{\cos(\pi g)+1}} & \frac{a\left(e^{2i\pi g}+2e^{i\pi g}+1\right)}{4\sqrt{\cos(\pi g)+1}} & \frac{a\left(1+2e^{-i\pi g}+e^{-2i\pi g}\right)}{4\sqrt{\cos(\pi g)+1}} & 0 & \\ \frac{ag\sin(\pi g)}{\sqrt{1-\cos(\pi g)}\sqrt{\cos(\pi g)+1}} & 1 & \frac{a\left(e^{2i\pi g}-2e^{i\pi g}+1\right)}{4\sqrt{1-\cos(\pi g)}} & \frac{a\left(1-2e^{-i\pi g}+e^{-2i\pi g}\right)}{4\sqrt{1-\cos(\pi g)}} & 0 & \\ -\frac{a\sqrt{\cos(\pi g)+1}}{2} & -\frac{a\sqrt{1-\cos(\pi g)}}{2} & ag\sin(\pi g) - iag\cos(\pi g) - i\sin(\pi g) - \cos(\pi g) & 0 & \frac{a(\sin(2\pi g)-i\cos & \\ -\frac{a\sqrt{\cos(\pi g)+1}}{2} & -\frac{a\sqrt{1-\cos(\pi g)}}{2} & 0 & ag\sin(\pi g) + iag\cos(\pi g) + i\sin(\pi g) - \cos(\pi g) & \frac{ia}{2} & \\ 0 & 0 & -\frac{ia}{2} & \frac{ia}{2} & ag\sin(\pi g) - iag\cos(\pi g) - i & \\ 0 & 0 & -\frac{ia}{2} & \frac{ia}{2} & 0 & \\ 0 & 0 & 0 & 0 & -\frac{\sqrt{2}ia}{2} & \\ 0 & 0 & 0 & 0 & 0 & \end{bmatrix} \tag{72}$$

We can ignore the $O(a)$ terms along the diagonal, we have,

$$\begin{bmatrix} -1 & \frac{ag\sin(\pi g)}{\sqrt{1-\cos(\pi g)}\sqrt{\cos(\pi g)+1}} & \frac{a\left(e^{2i\pi g}+2e^{i\pi g}+1\right)}{4\sqrt{\cos(\pi g)+1}} & \frac{a\left(1+2e^{-i\pi g}+e^{-2i\pi g}\right)}{4\sqrt{\cos(\pi g)+1}} & 0 & 0 & \\ \frac{ag\sin(\pi g)}{\sqrt{1-\cos(\pi g)}\sqrt{\cos(\pi g)+1}} & 1 & \frac{a\left(e^{2i\pi g}-2e^{i\pi g}+1\right)}{4\sqrt{1-\cos(\pi g)}} & \frac{a\left(1-2e^{-i\pi g}+e^{-2i\pi g}\right)}{4\sqrt{1-\cos(\pi g)}} & 0 & 0 & \\ -\frac{a\sqrt{\cos(\pi g)+1}}{2} & -\frac{a\sqrt{1-\cos(\pi g)}}{2} & -e^{i\pi g} & 0 & \frac{a(\sin(2\pi g)-i\cos(2\pi g))}{2} & -\frac{ia}{2} & \\ -\frac{a\sqrt{\cos(\pi g)+1}}{2} & -\frac{a\sqrt{1-\cos(\pi g)}}{2} & 0 & -e^{-i\pi g} & \frac{ia}{2} & \frac{a(\sin(2\pi g)+i\cos(2\pi g))}{2} & \\ 0 & 0 & -\frac{ia}{2} & \frac{ia}{2} & -e^{i\pi g} & 0 & \frac{\sqrt{2}a(\sin(2\pi g)-}{4} \\ 0 & 0 & -\frac{ia}{2} & \frac{ia}{2} & 0 & -e^{-i\pi g} & \frac{\sqrt{2}a(\sin(2\pi g)-}{4} \\ 0 & 0 & 0 & 0 & -\frac{\sqrt{2}ia}{2} & \frac{\sqrt{2}ia}{2} & ag\sin(\pi g) \\ 0 & 0 & 0 & 0 & 0 & 0 & ag\cos(\pi g) \end{bmatrix} \tag{73}$$

For the π mode we have,

$$\begin{bmatrix} 1 \\ -\frac{0.5ag\sin(\pi g)}{\sqrt{1-\cos(\pi g)}\sqrt{\cos(\pi g)+1}} \\ \frac{a\sqrt{\cos(\pi g)+1}}{2(1-e^{i\pi g})} \\ \frac{a\sqrt{\cos(\pi g)+1}e^{i\pi g}}{2e^{i\pi g}-2} \\ \frac{a^2\sqrt{\cos(\pi g)+1}}{4(e^{i\pi g}-1)\tan\left(\frac{\pi g}{2}\right)} \\ \frac{a^2\sqrt{\cos(\pi g)+1}e^{i\pi g}}{4(1-e^{i\pi g})\tan\left(\frac{\pi g}{2}\right)} \\ 0 \\ 0 \end{bmatrix}, \tag{74}$$

and for the zero mode we have,

$$\begin{bmatrix} \frac{ag\sin(\pi g)}{2\sqrt{1-\cos(\pi g)}\sqrt{\cos(\pi g)+1}} \\ 1 \\ -\frac{a\sqrt{1-\cos(\pi g)}}{2e^{i\pi g}+2} \\ -\frac{a\sqrt{1-\cos(\pi g)}e^{i\pi g}}{2e^{i\pi g}+2} \\ \frac{a^2\sqrt{1-\cos(\pi g)}\tan\left(\frac{\pi g}{2}\right)}{4(e^{i\pi g}+1)} \\ \frac{a^2\sqrt{1-\cos(\pi g)}e^{i\pi g}\tan\left(\frac{\pi g}{2}\right)}{4(e^{i\pi g}+1)} \\ 0 \\ 0 \end{bmatrix}. \tag{75}$$

We have similar relations to solve for,

$$\frac{ia}{2}\begin{pmatrix} -1 & 1 \\ -1 & 1 \end{pmatrix}\begin{pmatrix} \phi_{2n-1} \\ \phi_{2n} \end{pmatrix} = \begin{pmatrix} -e^{i\pi g}\pm 1 & 0 \\ 0 & -e^{-i\pi g}\pm 1 \end{pmatrix}\begin{pmatrix} \phi_{2n+1} \\ \phi_{2n+2} \end{pmatrix}. \tag{76}$$

With the only difference being the boundary conditions involving the first two components.

As we performed the approximate solution in the rotated basis we actually have,

$$V^\dagger \mathcal{W} V\psi \sim \epsilon\psi \tag{77}$$

$$\mathcal{W}(V\psi) \sim \epsilon(V\psi) \tag{78}$$

The zero modes are, (with $a = (g - (2n\pi)/T)$, small)

$$\begin{bmatrix} 1 \\ \frac{Ta}{2} \\ \frac{Ta}{2\tan\left(\frac{T}{2}\right)} \\ \frac{T^2a^2}{4\tan\left(\frac{T}{2}\right)} \\ \frac{T^2a^2}{4\tan^2\left(\frac{T}{2}\right)} \\ \frac{T^3a^3}{8\tan^2\left(\frac{T}{2}\right)} \\ \frac{T^3a^3}{8\tan^3\left(\frac{T}{2}\right)} \\ 0 \end{bmatrix}, \tag{79}$$

and the π modes are, (with $a = (g - ((2n+1)\pi)/T)$, small)

$$\begin{bmatrix} 1 \\ -\frac{Ta}{2} \\ \frac{Ta}{2\tan\left(\frac{T}{2}\right)} \\ -\frac{T^2a^2}{4\tan\left(\frac{T}{2}\right)} \\ \frac{T^2a^2}{4\tan^2\left(\frac{T}{2}\right)} \\ -\frac{T^3a^3}{8\tan^2\left(\frac{T}{2}\right)} \\ \frac{T^3a^3}{8\tan^3\left(\frac{T}{2}\right)} \\ 0 \end{bmatrix}. \tag{80}$$

The 0 mode in the $0-\pi$ phase, (with $a = T - \pi$, small),

$$\begin{bmatrix} \frac{\sqrt{2}(-ag\sin(\pi g)+2\cos(\pi g)+2)\sin(\pi g)}{4\sqrt{1-\cos(\pi g)}(\cos(\pi g)+1)} \\ \frac{\sqrt{2}(ag\sin(\pi g)-2\cos(\pi g)+2)}{4\sqrt{1-\cos(\pi g)}} \\ -\frac{a\sqrt{2-2\cos(\pi g)}}{4} \\ -\frac{\sqrt{2}a\sqrt{1-\cos(\pi g)}\tan\left(\frac{\pi g}{2}\right)}{4} \\ \frac{a^2\sqrt{2-2\cos(\pi g)}\tan\left(\frac{\pi g}{2}\right)}{8} \\ \frac{\sqrt{2}a^2\sqrt{1-\cos(\pi g)}\tan^2\left(\frac{\pi g}{2}\right)}{8} \\ 0 \\ 0 \end{bmatrix}, \tag{81}$$

and π mode in the $0-\pi$ phase, (with $a = T - \pi$, small),

$$\begin{bmatrix} \frac{\sqrt{2}(0.5ag\sin(\pi g)-\cos(\pi g)+1)\sin(\pi g)}{2(\cos(\pi g)-1)\sqrt{\cos(\pi g)+1}} \\ \frac{\sqrt{2}(-0.5ag\sin(\pi g)+\cos(\pi g)+1)}{2\sqrt{\cos(\pi g)+1}} \\ \frac{a\sqrt{2\cos(\pi g)+2}}{4} \\ -\frac{\sqrt{2}a\sqrt{\cos(\pi g)+1}}{4\tan\left(\frac{\pi g}{2}\right)} \\ -\frac{a^2\sqrt{2\cos(\pi g)+2}}{8\tan\left(\frac{\pi g}{2}\right)} \\ \frac{\sqrt{2}a^2\sqrt{\cos(\pi g)+1}}{8\tan^2\left(\frac{\pi g}{2}\right)} \\ 0 \\ 0 \end{bmatrix} \tag{82}$$

E. Strong mode in limiting cases

We turn off J_z and consider the following free drive,

$$U = e^{\frac{-iTJ_xH_{xx}}{2}} e^{\frac{-iTgH_z}{2}}. \tag{83}$$

Now we consider the following simple cases:

- $Tg = (2n+1)\pi$, TJ_x arbitrary: $e^{-iTg/2H_z} \propto \mathbb{Z}_2$, thus $U^\dagger\sigma_1^xU = \mathbb{Z}_2\sigma_1^x\mathbb{Z}_2 = -\sigma_1^x$, a SPM, there is no SZM. If we start the Arnoldi iteration, we have $|1) = \sigma_1^x$ and we now look for $|2)$.

$$|2') = \mathcal{W}|1) = -|1) \tag{84}$$

Thus the Krylov subspace terminates after the frist basis vector $|1) = \sigma_1^x$, $\mathcal{W}$ is a "matrix" with a single element, -1. This will give us the SPM flipping behavior we want.

- $Tg = (2n)\pi$, TJ_x arbitrary: Now $e^{-iTg/2H_z} \propto 1$, thus $U^\dagger\sigma_1^xU = \sigma_1^x$. We have a SZM, there is no SPM. Follow the same steps in the above section, its clear that $\mathcal{W} = 1$.

- $TJ_x = (2n+1)\pi$,Tg arbitrary: Now we have $e^{-iTJ_x/2H_{xx}} \propto \sigma_1^x\sigma_L^x$. With $e^{-iTg/2H_z} =$

$\prod_l [\cos(Tg/2) - i\sigma_l^z \sin(Tg/2)]$ it is straightforward to check,

$$U^\dagger \sigma_1^x U = \cos(Tg)\sigma_1^x - \sin(Tg)\sigma_1^y \tag{85}$$

$$U^\dagger \sigma_1^y U = -\sin(Tg)\sigma_1^x - \cos(Tg)\sigma_1^y. \tag{86}$$

We now construct our Krylov subspace for σ_1^x, beginning with $|1) = \sigma_1^x$. We then have,

$$\mathcal{W}|1) = \cos(Tg)\sigma_1^x - \sin(Tg)\sigma_1^y, \tag{87}$$

giving,

$$|2') = \mathcal{W}|0) - \cos(Tg)|0) = -\sin(Tg)\sigma_1^y, \tag{88}$$

thus after normalization,

$$|2) = -\sigma_1^y. \tag{89}$$

From the above we know $\mathcal{W}|2)$ will be a linear combination of $|1), |2)$, we have,

$$\mathcal{W} \to \begin{pmatrix} \cos(Tg) & |\sin(Tg)| \\ |\sin(Tg)| & -\cos(Tg) \end{pmatrix}, \tag{90}$$

which is just rehashing what we already have above.

- $TJ_x = 2n\pi$ and Tg arbitrary: We have $e^{-iTJ_x/2H_{xx}} \propto 1$ and no strong modes exist unless $Tg = \mathbb{Z}\pi$. If $Tg = 2n\pi$ then σ_1^x is a SZM, in this case $U \propto 1$ so it is trivially a SZM, $\mathcal{W} = 1$. If $Tg = (2n+1)\pi$, then σ_1^x is a SPM, $U \propto \mathbb{Z}_2$ and we have $\mathcal{W} = -1$ If $Tg \neq \mathbb{Z}\pi$, then $U^\dagger \sigma_1^x U = c_1\sigma_1^x + c_2\sigma_1^y$ and likewise for $x \leftrightarrow y$. Thus the Krylov subspace for σ_1^x is 2 dimensional and we again have a 2×2 matrix $\mathcal{W}$. However, this time the spectrum will not yield eigenvalues ± 1 and instead will be generic phases.

III. LANCZOS METHOD

Another alternative is to simply find H_F and perform Lanczos on σ_1^x as before,

$$H_F = \frac{i}{T}\log(U). \tag{91}$$

Fig. 4 performs Lanczos on with H_F as calculated above in the interacting case. We see the b_n vary considerably from what we are used to in the static case. The main differences being the pattern of staggering is no longer like an SSH model and the "plateaus" are no long increasing with system size. The latter can be explained as the manybody quasienergy spectrum is bounded by definition of the logarithm. A bounded spectrum will produce bounded b_n CITE BOOK. The former difference is a little more interesting as we can no longer use our standard edge states to approximate the 0-π ASMs.

A. Free case

Now we consider the free case of Lanczos with H_F. Fig. 5 considers Lanczos for the free case in a couple different ways. The first method is to enter the Majorana basis and to consider the Lanczos method there, using the dynamics generated by M in Eq. (22). Here, the Lanczos method is a simple basis rotation and the spectrum of H_K, the Krylov Hamiltonian, will be exactly the same as that of Eq. (22). That is, we begin with a single-particle propagator M, and we end with a single-particle propagator $\mathcal{L}$, so there is no subtleties with branch cuts, the branch cut of M, is equivalent to the branch cut of H_K.

The second way to perform Lanczos in the free basis is to work in the many-body spin basis and simply turn off J_z. In this case, we are performing a branch cut on the many-body H_F, not the single-particle spectrum. This has no impact on the dynamics as the bottom of Fig. 5 shows they are equivalent. However, the center and top rows of Fig. 5 show that the spectrum of H_K and the b_n are sensitive to whether the branch cut is performed on the level of the many-body spectrum versus the single-particle spectrum.

In Fig. 5, the blue data set corresponds Lanczos performed with H_F without any special treatment for the single-particle status of the problem. The seed state is σ_1^x and after $2L$ iterations of the Lanczos algorithm, it terminates after exhausting all of the Krylov space of σ_1^x. We see the resulting spectrum of H_K extends beyond the FBZ as indicated by the red lines. The b_n are shown in the top row and share little in common with the b_n from the previous works.

We can now wrap the blue spectrum of H_K such that it fits within the FBZ, which is now given by the green data set. The resulting b_n of this new H_K are shown in the top panel. We note that this wrapping of the spectrum requires being in the diagonal basis which will typically not be possible for us. We see the green b_n of the top row match the b_n from the free Lanczos performed in the single-particle basis, where the spectrum wrapping is unessary.

As touched upon in the previous paragraph, to align the Majorana free picture and the spin free picture, we needed to wrap the spectrum of H_K, requiring the diagonalization of H_K. This is only possible in the free case, were we can easily find the full Krylov subspace of our seed operator. For the interacting case, we will have to cut off the Lanczos algorithm and thus we have a truncated H_K, which is not a proper quantity to diagonalize.

IV. BRANCH CUTS

Consider time evolution with a static H, for some period T, the goal is to obtain the Lanczos coefficients of $H_F = H$ in some general way. We only know $U = \exp -iTH$, thus $H_F = i\log(U)$ will involve folding the

FIG. 4: b_n determined from Floquet Hamiltonian. From top to bottom, left to right we have $T = .5, 1.5, 3.6, 5.0, 8.25$. This corresponds to ASZM,ASZM,ASZPM,trivial,ASPM. The first ASZM is very high frequency drive (off resonant with many-body spectrum). The b_n are different from the static case, the current belief is that since the quasienergy spectrum is bounded, the resulting b_n are bounded.

spectrum.

We start with the seed operator O, we can consider the diagonal basis of H_F,

$$O \to \tilde{O}, H_F \to D_F. \tag{92}$$

We have,

$$\mathcal{L}O = [H, O] \to [D_F, \tilde{O}]. \tag{93}$$

We can further decompose D_F,

$$D_F = D_H + D_Z, \tag{94}$$

where D_H are the energy levels of the static Hamiltonian and D_Z are the shifts in quasienergy needed to keep the many body spectrum within the corresponding branch cut of the logarithm. However, we do not know either D_H nor D_Z.

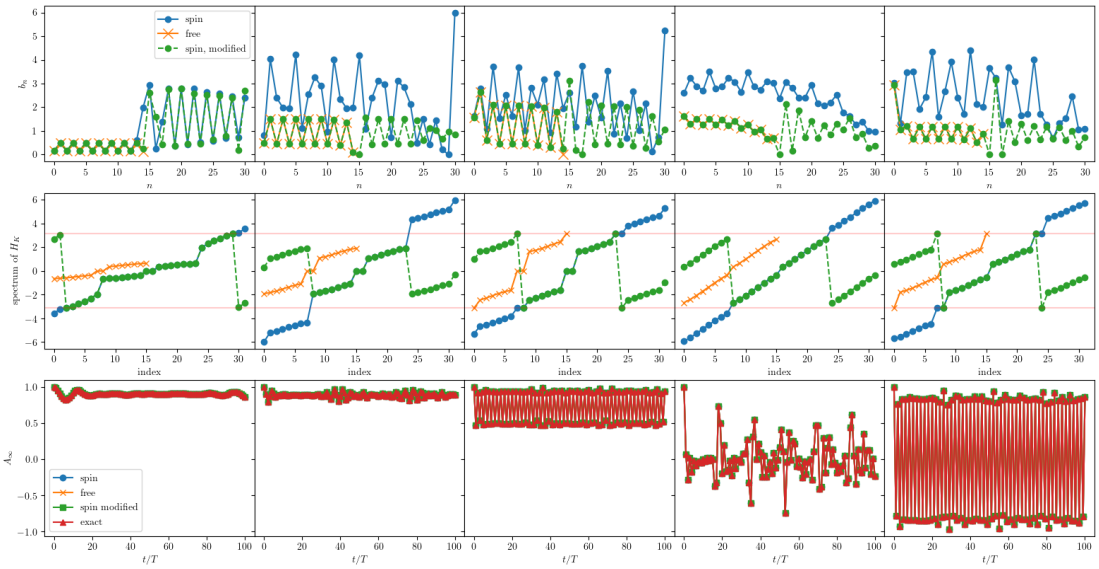

FIG. 5: All free, phases as before, left to right $T = .5, 1.5, 3.6, 5, 8.25$. Looking into the difference between the spin basis and the majorana basis. The red data in the bottom row is the exact result.

We attempted to expand the Lanczos algorithm,

$$[D_H + D_z, \tilde{O}_1] = b_1 \tilde{O}_2 \tag{95}$$

$$[D_H + D_z, \tilde{O}_2] = b_2 \tilde{O}_3 + b_1 \tilde{O}_1 \tag{96}$$

$$\rightarrow p[D_H, [D_H, \tilde{O}_1]] + [D_z, [D_z, \tilde{O}_1]] + 2[D_H, [D_Z, \tilde{O}_1]] = b_1 b_2 \tilde{O}_3 + b_1^2 \tilde{O}_1, \tag{97}$$

where in the last line we multiplied by b_1 on both sides and used the fact $[D_H, D_Z] = 0$.